Electron scattering and bound-state energies in crossed N-chain wires. A comparative study of discrete and continuous models

1992 J. Phys.: Condens. Matter 4 7103

(http://iopscience.iop.org/0953-8984/4/34/009)

J. Phys.: Condens. Matter 4 (1992) 7103–7114. Printed in the UK

Electron scattering and bound-state energies in crossed N-chain wires. A comparative study of discrete and continuous models

Yu B Gaididei, L I Malysheva and A I Onipko
Bogolyubov Institute for Theoretical Physics, Kiev 143, 252143, Ukraine

Received 23 May 1992

Abstract. A closed set of equations, which describe electron scattering in a right-angle intersection of two 2D wires, is derived on the basis of the tight-binding Hamiltonian with the interaction between the neighbouring lattice sites. In the continuum limit, $N \to \infty$, Na = constant (N is the number of coupled chains that constitute each wire, a is the lattice constant), the equations are shown to be identical to those known in the matching theory for the continuous version of the model. An analytic solution of the scattering problem obtained yields the scattering amplitude of the single-mode electron-wave propagation and the equations determining the bound-state energies of the system. It is shown that the bound-state to band-state energy gap has a qualitatively different dependence on N (i.e. on wire width) in the cases of even- and odd-parity bound states. The effect reveals itself in ultra-narrow channels, $N \leqslant 10$. The width dependence of the reflection and transmission probabilities in crossed ultra-narrow wires is also discussed.

1. Introduction

Much attention has recently been paid to the wave-like electron transport in various two-dimensional (2D) geometries regarded as promising for nanoelectronics (see [1–7] and references therein). The objective in these studies was to understand the behaviour of electrons in quantum-size structures and to estimate the possibility of implementing electronic devices and integrated designs based on quantum-mechanics effects. This field of activities has become of practical importance due to the fast progress in nanometer-scale technology.

Here we address the problem of ballistic (or coherent) electron transport through a right-angle intersection of N-chain wires. In contrast to the earlier work on the subject [1], which is based on the effective-mass Hamiltonian and consequently only refers to the continuous model of crossed wires, we use the tight-binding formalism, which has much wider applications and accounts for the discrete nature of real structures. In particular, we are able to investigate, in the framework of our approach, the properties of a system built up of an arbitrary number of chains (which is of interest to molecular electronics) and to identify the changes in transport characteristics, varying the wire width from its minimal value to infinity. Obviously, the continuous model is not appropriate for 'narrow' channels. One of the important questions to be answered here is, therefore, what 'narrow' really means in the context of the bound-state spectrum and the electron-transport characteristics of crossed wires.

0953-8984/92/347103+12$04.50

Note that the tight-binding formalism has recently been applied to computational treatment of a similar problem of electron transport in wires with a side stub [2]. In this paper we show that the principal characteristics of wire crossing and related structures can be described quite accurately by analytic expressions, at least within and near the first-mode band.

The paper is organized as follows. In section 2 we derive a set of basic equations for the scattering problem in crossed wires and show that the discrete model in the continuum limit is equivalent to the continuous one. For this purpose, a continuous version of the basic equations is rederived in the appendix. In section 3, the energies of the ground state and the excited bound states in crossed wires with different chain numbers are calculated and compared with the corresponding results for the continuous model. Section 4 is devoted to the characteristics of the fundamental-mode propagation and section 5 concludes the discussion with a brief summary of the main results.

2. Basic equations

To describe the system we use the standard one-electron Hamiltonian

$$H = -4L\sum_{\boldsymbol{R}} a_{\boldsymbol{R}}^{+}a_{\boldsymbol{R}} + L\sum_{\boldsymbol{R},\delta\boldsymbol{R}} a_{\boldsymbol{R}}^{+}a_{\boldsymbol{R}+\delta\boldsymbol{R}} \tag{1}$$

where $a_{\boldsymbol{R}}^{+}$ and $a_{\boldsymbol{R}}$ are the Fermi operators of crealtion and annihilation, respectively, of an electron on a site $\boldsymbol{R}$. Possible values of $\boldsymbol{R}$ and $\delta\boldsymbol{R}$ (the latter connects the site $\boldsymbol{R}$ with its nearest neighbours) are defined in the schematic representation of the crossed wires in figure 1. Each region of the system labelled with 'left', 'right', 'up', 'down' and 'in' has an independent numbering of the lattice sites $m, n = \boldsymbol{R}$. An electron's potential is infinite outside the lattice outlined in figure 1 as well as outside the picture plane. For the convenience of comparison (in the continuum limit) with the effective-mass approximation, the electron energy on the site $\boldsymbol{R}$ is set to be equal to $-4L$. In the latter case, the electron resonant transfer energy is $L = -\hbar^2/(2m^*a^2)$, where a is the lattice constant and m^* is the effective electronic mass in the wires. In terms of the effective-mass Hamiltonian just defined, an electron inside the wires is free and, in the classic sense, unbound.

The solution of the time-independent Schrödinger equation

$$H\Psi = E\Psi \tag{2}$$

which determines the scattering behaviour in crossed wires, can be presented in the form

$$\Psi_\gamma = \sum_{m,n\in\boldsymbol{R}_\gamma} \psi_{m,n}^{\gamma} a_{m,n}^{+}|0\rangle \tag{3}$$

for each of the labelled regions. The expansion coefficients $\psi_{m,n}^{\gamma}$ with $\gamma = \mathrm{l}, \mathrm{r}, \mathrm{up}, \mathrm{d}$ are

$$\psi_{m,n\in\boldsymbol{R}_\mathrm{l}}^{\mathrm{l}} = \sqrt{\frac{2}{N+1}}\left(\exp(-\mathrm{i}k_{j_0}n)\sin(\chi_{j_0}m)\right.$$

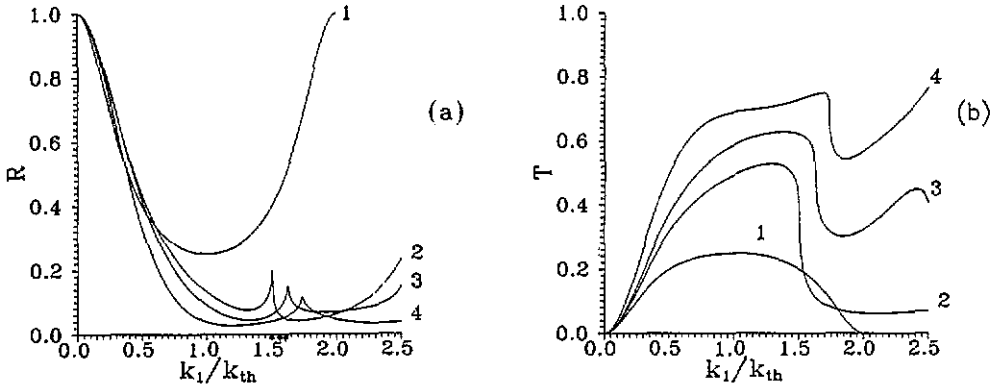

Figure 1. Schematic diagram of the lattice arrangement in crossed N-chain wires. The numbering of the lattice sites, m, n, is independent for each of the labelled regions. In the 'left' and 'right' regions, $m = \overline{1,N}$, $n = 1,2,\ldots$; in the 'up' and 'down' regions, $m = 1,2,\ldots$, $n = \overline{1,N}$; and $m = \overline{1,N}$, $n = \overline{1,N}$ in the 'in' region. a is the periodicity of the lattice. The full lines show the boundaries of the wires in the continuum limit, $N \to \infty$, $Na = \text{const}$. In this case the wire width is $w = (N+1)a$, N being the wire width in the site number.

$$+ \sum_{j=1}^{N} r_{k_j} \exp(ik_j(n-1)) \sin(\chi_j m)\Big) \tag{4}$$

$$\psi^{r}_{m,n\in R_r} = \sqrt{\frac{2}{N+1}} \sum_{j=1}^{N} t^{r}_{k_j} \exp(ik_j(n-1)) \sin(\chi_j m) \tag{5}$$

$$\psi^{up}_{m,n\in R_{up}} = \sqrt{\frac{2}{N+1}} \sum_{j=1}^{N} t^{up}_{k_j} \exp(ik_j(m-1)) \sin(\chi_j n) \tag{6}$$

$$\psi^{d}_{m,n\in R_d} = \sqrt{\frac{2}{N+1}} \sum_{j=1}^{N} t^{d}_{k_j} \exp(ik_j(m-1)) \sin(\chi_j n). \tag{7}$$

In equations (4)–(7), $\chi_j = \pi j/(N+1)$ is the quantum number of the transverse electron motion and k_j is the longitudinal wave vector of the jth mode. The mode number j_0 and the wave vector k_{j_0} determine the energy of the incident electrons (in the left-hand region)

$$E = 2L(\cos(k_{j_0}) + \cos(\chi_{j_0}) - 2). \tag{8}$$

The rest of k_j and χ_j in the expansions (4)–(7) (including evanescent modes, for which the wave vectors are imaginary, $k_j \to ik_j$) are determined by the energy conservation law

$$\cos(k_{j_0}) + \cos(\chi_{j_0}) = \cos(k_j) + \cos(\chi_j). \tag{9}$$

The wave function (3)–(7) satisfies equation (2) in the regions 'left', 'right', 'up' and 'down' except at the boundaries of the region of intersection, where the

Schrödinger equation is

$$\delta_{j,j_0} + \exp(-ik_j)r_{k_j} = \sqrt{\frac{2}{N+1}} \sum_{m=1}^{N} \sin(\chi_j m)\psi^{\text{in}}_{m,1} \tag{10}$$

$$\exp(-ik_j)t^{\text{r}}_{k_j} = \sqrt{\frac{2}{N+1}} \sum_{m=1}^{N} \sin(\chi_j m)\psi^{\text{in}}_{m,N} \tag{11}$$

$$\exp(-ik_j)t^{\text{up}}_{k_j} = \sqrt{\frac{2}{N+1}} \sum_{n=1}^{N} \sin(\chi_j n)\psi^{\text{in}}_{1,n} \tag{12}$$

$$\exp(-ik_j)t^{\text{d}}_{k_j} = \sqrt{\frac{2}{N+1}} \sum_{n=1}^{N} \sin(\chi_j n)\psi^{\text{in}}_{N,n}. \tag{13}$$

On the other hand, in the region of intersection the Schrödinger equation can be solved formally using the Lifshitz method [8]. As a result, the expansion coefficients $\psi^{\text{in}}_{m,n}$ are connected with r_{k_j} and $t^{\gamma}_{k_j}$ by the equations

$$\begin{aligned}\sqrt{\frac{N+1}{2}}\psi^{\text{in}}_{m,n} &= g_{n,1}(j_0)\sin(\chi_{j_0}m)\exp(-ik_{j_0}) \\ &+ \sum_{j=1}^{N}(\sin(\chi_j m)[r_{k_j}g_{n,1}(j) + t^{\text{r}}_{k_j}g_{n,N}(j)] \\ &+ \sin(\chi_j n)[t^{\text{up}}_{k_j}g_{m,1}(j) + t^{\text{d}}_{k_j}g_{m,N}(j)])\end{aligned} \tag{14}$$

where

$$g_{m,n}(j) = \frac{1}{N+1}\sum_{j'=1}^{N}\frac{\sin(\chi_{j'}m)\sin(\chi_{j'}n)}{\cos(k_j) - \cos(\chi_{j'})}. \tag{15}$$

Making use of equation (14) in equations (10)–(13) we finally get, after some obvious algebra,

$$\begin{aligned}\exp(-i(N+1)k_j)r_{k_j} &= -\delta_{j,j_0}\exp(iNk_j) + t^{\text{r}}_{k_j} + \frac{\sin((N+1)k_j)}{\sin(k_j)} \\ &\times \sum_{j'=1}^{N} G_{j,j'}(t^{\text{up}}_{k_{j'}} + (-1)^{j+1}t^{\text{d}}_{k_{j'}})\end{aligned} \tag{16}$$

$$\begin{aligned}\exp(-i(N+1)k_j)t^{\text{r}}_{k_j} &= \delta_{j,j_0}\exp(-ik_j) + r_{k_j} + \frac{\sin((N+1)k_j)}{\sin(k_j)} \\ &\times \sum_{j'=1}^{N}(-1)^{j'+1}G_{j,j'}(t^{\text{up}}_{k_{j'}} + (-1)^{j+1}t^{\text{d}}_{k_{j'}})\end{aligned} \tag{17}$$

$$\begin{aligned}\exp(-i(N+1)k_j)t^{\text{up}}_{k_j} &= t^{\text{d}}_{k_j} + \frac{\sin((N+1)k_j)}{\sin(k_j)}\Big(\exp(-ik_{j_0})G_{j,j_0} \\ &+ \sum_{j'=1}^{N} G_{j,j'}(r_{k_{j'}} + (-1)^{j+1}t^{\text{r}}_{k_{j'}})\Big)\end{aligned} \tag{18}$$

$$\exp(-i(N+1)k_j)t^{d}_{k_j} = t^{up}_{k_j} + \frac{\sin((N+1)k_j)}{\sin(k_j)}((-1)^{j_0+1}\exp(-ik_{j_0})G_{j,j_0} + \sum_{j'=1}^{N}(-1)^{j'+1}G_{j,j'}(r_{k_{j'}} + (-1)^{j+1}t^{r}_{k_{j'}})) \tag{19}$$

where

$$G_{j,j'} = \frac{1}{N+1}\frac{\sin(\chi_j)\sin(\chi_{j'})}{\cos(k_j) - \cos(\chi_{j'})}. \tag{20}$$

In the continuum limit, it is natural to introduce a new wave vector $q_j = k_j/k_{th}$ related to the current-threshold wave vector $k_{th} = \pi/(N+1)$. Then, taking the limit $N \to \infty$, Na =constant, we need to make the following changes in the coefficients of equations (16)–(19): $(N+1)k_j \to \pi q_j$, $\exp(ik_j) \to 1$, $\sin(k_j) \to q_j$, $G_{j,j'} \to G^{c}_{j,j'} = (2jj'/(\pi(j'^2 - q_j^2))$. After the transformations outlined, the set of equations (15)–(19) coincides with equations (A5)–(A8) obtained for the continuous model (see appendix).

The comparison just made proves that the continuous model is completely equivalent to its discrete analogue in the continuum limit. Evidently, the discrete model is more general and yet easier to handle.

To conclude this section, we note that the above equations can be applied to structures of both T- and L-type. Setting, for instance, $t^{r}_{k_j}$ or $t^{d}_{k_j}$ to be zero, we obtain the case of a T structure for two different configurations of the scattering process. Equations for the L structure (the right-angle bend) follow from equations (15)–(19) if $t^{r}_{k_j} = t^{d}_{k_j} = 0$.

3. Discrete levels in a crossed-wires system

The components of the scattering amplitude r_{k_j} and $t^{\gamma}_{k_j}$ determine the probabilities of finding an electron in a certain region with the wave vector k_j in the jth mode and, additionally, the bound-state energies of the system. These energies manifest themselves as the poles of the scattering amplitude [9].

The existence of discrete levels, which correspond to the ground (even-parity) bound state and to the excited odd-parity bound state in the continuous model, was predicted by Schult *et al* [1]. They solved the spectral problem directly, using computational methods. Here, we can look at the equations which allow one to investigate both the continuous and the discrete models.

To get an analytic solution, we truncate the set (15)–(19) on the sixth mode. Equating the denominators of r_{k_1} and r_{k_2} to zero (none of the other r_{k_j} and $t^{\gamma}_{k_j}$ give extra poles), we get the following equations (in the six-mode approximation):

$$Z_1^{+} = F_1(Q^{od+}_{j,j'}) \tag{21}$$

$$Z_2^{-} = F_2(Q^{ev-}_{j,j'}) \tag{22}$$

where

$$F_1(Q^{od+}_{j,j'}) = Q^{od+}_{1,1} + \frac{[Q^{od+}_{1,3} + Q^{od+}_{1,5}Q^{od+}_{5,3}/(Z_5^{+} + Q^{od+}_{5,5})]^2}{Z_3^{+} - Q^{od+}_{3,3} - (Q^{od+}_{3,5})^2/(Z_5^{+} - Q^{od+}_{5,5})} + \frac{(Q^{od+}_{1,5})^2}{Z_5^{+} - Q^{od+}_{5,5}} \tag{23}$$

$$F_2(Q^{ev-}_{j,j'}) = Q^{ev-}_{2,2} + \frac{[Q^{ev-}_{2,4} + Q^{ev-}_{2,6}Q^{ev-}_{6,4}/(Z^-_6 - Q^{ev-}_{6,6})]^2}{Z^-_4 - Q^{ev-}_{4,4} - (Q^{ev-}_{4,6})^2/(Z^-_6 - Q^{ev-}_{6,6})} + \frac{(Q^{ev-}_{2,6})^2}{Z^-_6 - Q^{ev-}_{6,6}} \tag{24}$$

$$Q^{od+}_{j,j'} = 4\sum_{j''=1,3,5} \frac{G_{j,j''}G_{j'',j'}}{Z^+_{j''}} \qquad Q^{ev-}_{j,j'} = 4\sum_{j''=2,4,6} \frac{G_{j,j''}G_{j'',j'}}{Z^-_{j''}} \tag{25}$$

$$Z^+_j = \frac{\sinh(k_j)\exp(\frac{1}{2}(N+1)k_j)}{\cosh(\frac{1}{2}(N+1)k_j)} \qquad Z^-_j = \frac{\sinh(k_j)\exp(\frac{1}{2}(N+1)k_j)}{\sinh(\frac{1}{2}(N+1)k_j)}. \tag{26}$$

In the continuum limit, the quantities Z_j and $Q_{j,j'}$ should be redefined according to the rules formulated above.

Equation (21) determines the ground-state energy E_1 and equation (22) the excited bound-state energy E_2. These equations are exact if $N \leqslant 6$. If we use them for one-, two-, ..., and five-chain wires, we need to omit the terms which contain indices 2 to 6, 3 to 6, ... and 6, respectively. Note that the even modes do not contribute to E_1, and that odd modes do not contribute to E_2.

Let us consider first the solution of equation (21) in the continuum limit. In the one-mode approximation it reduces to

$$\frac{2}{\pi}\frac{1+\exp(-\pi q_1)}{q_1(q_1^2+1)} = 1$$

which gives $q_1 = 0.5646$ and we obtain for the ground-state energy $(E_1^{(1)} - E_{1th})/E_{1th} = \Delta E_1^{(1)} = -0.319$, where $E_{1th} = E(k_1 = 0) = \hbar^2\pi^2/(2m^*w^2)$ is the current-threshold energy, i.e. the bottom of the continuous spectrum of the system, and $w = (N+1)a$. The correct value of ΔE_1 is -0.34 [1]. Thus, the contribution of the third and higher modes into the ground-state energy is only about six per cent. In particular, $\Delta E_1^{(3)} = -0.331$, $\Delta E_1^{(5)} = -0.335$.

The roots of equation (21) (the unknown now is $\cosh(k_1)$) give the exact values of E_1 in a crossed N-chain-wire system with $N = 1, 2, \ldots, 6$. For $N > 6$, $E_{1,2}(N)$ calculated in accordance with equations (21) and (22) are accurate to within three per cent or better. The results are presented in table 1, where for the sake of convenience we use two different energy units E_{1th} (as for the continuous model) and $2|L|$. Surprisingly, the continuous model gives the right order of ΔE_1 even in crossed chains, $N = 1$. Still, if $N < 10$, the difference $E_1(N) - E_1^{CL}$ is far from negligible (see table 1). It is also worth emphasizing that the correct definition of the wire width is not $(N-1)a$, as could be intuitively expected, but $(N+1)a$. The case $N = 1$ deserves special attention because it brings to light the nature of the bound state. Indeed, the discrete state in a crossed-chains system arises because the intersection site, which has four nearest-neighbour sites, is not equivalent to all the other sites. In a sense, it is a perturbed site. Therefore, the situation with bound states of a crossed-wires system is very similar to that of defect states in solids. In the case of finite-width crossed wires, the role of the perturbed sites is played by the corner sites of the intersection region, as was demonstrated in wave-function terms in [1].

The position of the excited bound-state level E_2 is determined by equation (22), which can be rewritten in the continuum limit in the two-mode approximation as

$$\frac{8}{\pi}\frac{1-\exp(-\pi q_2)}{q_2(q_2^2+4)} = 1.$$

Its solution is $q_2 = 0.4632$ and we get $\Delta E_2^{(2)} = (E_2^{(2)} - E_{2\text{th}})/E_{1\text{th}} = -0.215$. Comparing this value with $\Delta E_2 = -0.28$ [1], we see that the lowest approximation does not work as well as for E_1. Making two further steps, $\Delta E_2^{(4)} = -0.249$, $\Delta E_2^{(6)} = -0.262$, we obtain a good agreement with the Schult, Ravenhall and Wyld computational result.

Our calculations show that the odd-parity state appears first in the three-chain system at the edge of the second-mode band, i.e. $\Delta E_2(3) = 0$. The state separates from the band in the four-chain system, $\Delta E_2(4) = -0.032$ (in the units of $E_{1\text{th}}$) (see table 1). Reasons for the absence of this state in the case of $N < 4$ are easily understood by noting that the wave function of the odd-parity bound state is zero in the middle of the intersection region.

Table 1. Discrete levels in the crossed N-chain wires. $|\Delta E_{1(2)}|$ is the separation of an even-parity (odd-parity) bound state from the bottom of the first- (second-) mode band, $\Delta E_{1(2)} = E_{1(2)} - E_{1(2)\text{th}}/E_{1\text{th}}$, $E_{1(2)\text{th}} = E(k_{1(2)} = 0)$. $E_{1\text{th}}$, the current-threshold energy, is taken equal to $\hbar^2\pi^2[2m^*a^2(N+1)^2]^{-1}$. For $N > 6$, $\Delta E_{1,2}$ is calculated in the six-mode approximation.

N	$-\Delta E_1$	$-\Delta E_1 E_{1\text{th}}/\|2L\|$	$-\Delta E_2$	$-\Delta E_2 E_{1\text{th}}/\|2L\|$
1	0.125	0.154	—	—
2	0.215	0.118	—	—
3	0.261	0.0796	0	0
4	0.281	0.0555	0.032	0.0062
5	0.294	0.0405	0.074	0.0102
6	0.305	0.0307	0.11	0.0111
7	0.310	0.0240	0.138	0.0106
8	0.316	0.0193	0.159	0.0097
9	0.318	0.0158	0.176	0.0087
10	0.322	0.0131	0.189	0.0077
20	0.333	0.0037	0.246	0.0028
CL†	0.335	0	0.262	0
CL [1]	0.34	0	0.28	0

† CL — the continuum limit.

The dependence $E_2(N)$, as distinct from the ground-state energy, in the intersection of narrow channels differs drastically from the $1/w^2$ law predicted by the continuous model. The function $|\Delta E_2(N)|$, if non-scaled (i.e. in its natural units $2|L|$ but not in units of $E_{1\text{th}}$), is non-monotonic and has a minimum at $N = 6$. For this reason, deviations from the $1/w^2$ law in $\Delta E_2(N)$ become pronounced for wire widths appreciably greater than in the case of the ground state.

The results for the discrete model discussed above refer to the bound states in the lower part of the spectrum (if $L < 0$). The continuous spectrum of the discrete system is restricted and, therefore, symmetric bound states appear in the upper part of the spectrum: E_1 has its counterpart above the highest odd band and that of E_2 is above the highest even band. Thus, the highest state in the crossed-wires system with even (odd) N is the odd- (even-) parity bound state whose energy is above the continuous spectrum of the system.

4. Scattering probabilities for the fundamental-mode propagation

Only the first-mode electron wave can propagate in the system in the energy interval

$$\cos(2k_{th}) - 1 \leqslant \frac{E}{2L} = \cos(k_1) + \cos(k_{th}) - 2 \leqslant \cos(k_{th}) - 1$$

(for the continuous model, $k_{th} \leqslant \sqrt{k_1^2 + k_{th}^2} \leqslant 2k_{th}$). Since mode-transforming processes are forbidden, the fundamental-mode propagation is especially useful for applications. Note that for 30 nm wire width and an effective mass $m^* = 0.05m_e$, the first-mode band covers the interval kT at room temperature.

As in the preceding section, we use the solution of equations (15)–(19) in the six-mode approximation to find the scattering probabilities of reflection (R), forward transmission (T) and side transmission (S)

$$r_{k_1} = \tfrac{1}{2}(X^+_{k_1} + X^-_{k_1}) \qquad t^r_{k_1} = \tfrac{1}{2}(X^+_{k_1} - X^-_{k_1}) \tag{27}$$

where

$$X^{+(-)}_{k_1} = e^{-ik_1}\frac{+(-)Z_1^{+(-)}\exp(i(N+1)k_1) + F_1(Q^{od(ev)+}_{j,j'})}{Z_1^{+(-)} - F_1(Q^{od(ev)+}_{j,j'})}. \tag{28}$$

The functions F_1 and $Q^{od+}_{j,j'}$, $Q^{ev+}_{j,j'}$ are defined in equations (23) and (25), respectively (with $-$ replaced by $+$). The wave vectors k_j in equations (25) and (26) should be interpreted as ik_1 for $j = 1$ and k_j for $j > 1$. (In the case of second-mode propagation, k_j are ik_1, ik_2 for $j = 1,2$ and k_j for $j > 2$.) To obtain the exact expressions for the scattering amplitude in N-chain crossed wires with $N = 1, 2, \ldots, 5$, one should, as above, omit the terms with the indices 2 to 6, 3 to 6, ..., and 6, respectively.

The dependences $R(k_1) = |r_{k_1}|^2$, $T(k_1) = |t^r_{k_1}|^2$ ($S(k_1) = 1 - R - T$), calculated in accordance with equations (27) and (28), are displayed in figure 2 to show how the transport characteristics are transformed between the limiting cases $N = 1$ and $N \gg 1$. It is clear that if $N \geqslant 9$, the characteristics of the fundamental-mode propagation in crossed wires as functions of k_1/k_{th} depend rather weakly on the chain number. Even the curves that correspond to $N = 3$ are not very much different from those calculated in the continuum limit (see figure 2). The only exceptions in this sense are the cases of $N = 1, 2$.

5. *Discussion*

We consider the scattering problem in crossed 2D N-chain wires viewed as a square-lattice atomic arrangement with each site atom coupled to its nearest neighbours via the electron resonant-transfer interaction. In this way, the discrete nature of real electron channels is taken into account. At the same time, the continuous analogue of the model studied previously [1] is also included as a particular limiting case. An obvious advantage gained is the possibility to follow the dependences of the bound-state energies $E_{1,2}$ and the scattering probabilities on width down to the minimal wire width, $N = 1$ ($w = 2a$). The continuous model predicts for the crossed wires (and similar discontinuities) $E_{1,2} \sim 1/w^2$. It thus reveals a disappointing property: $E_{1,2}$ tends to infinity as w tends to zero — the classical minimal width. This unphysical result is removed simply in our approach, owing to the correct definition of the minimal wire width.

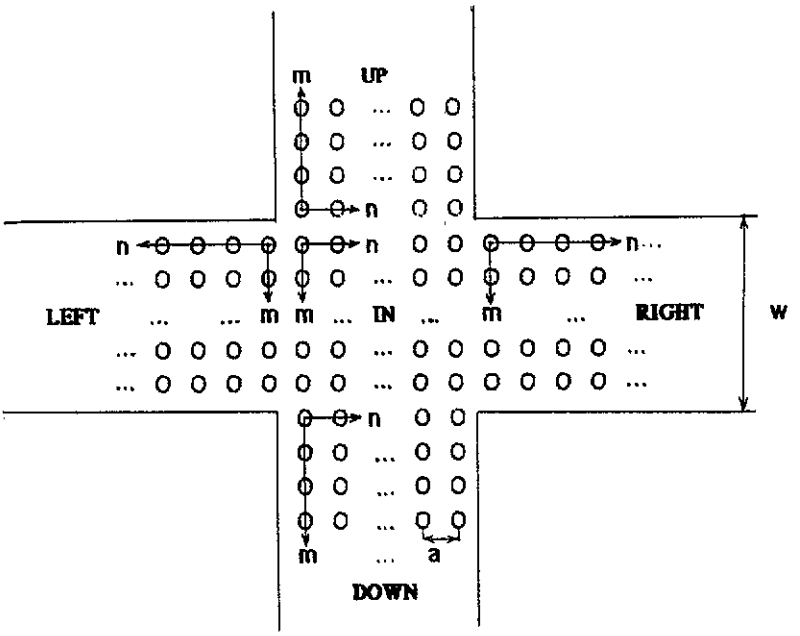

Figure 2. Ballistic transport characteristics in the crossed-wire system as functions of the electron's longitudinal wave vector k_1 for different numbers of chains in the wires. (*a*) R is the reflection probability of the crossing, and (*b*) T is the forward-through-crossing transmission probability. The chain number N equals 1, 2, 3, 9 for the curves 1, 2, 3, 4, respectively. The values of k_1 that satisfy the equation $\cos(k_1)+\cos(k_{th})-\cos(2k_{th})=1$ correspond to the opening of the second-mode propagation. These values are indicated by arrows: $k_1/k_{th}=1.5$ $(N=2)$, $k_1/k_{th}=1.621$ $(N=3)$, $k_1/k_{th}=1.717$ $(N=9)$ $(k_{th}=\pi/(N+1))$. On the scale given, R and T for $N=9$ (curves 4(*a*) and (*b*)) are undistinguishable from those in the continuum limit.

The ground-state energy in units of E_{1th} is nearly constant, down to the channel width $\sim$ 25 nm (for the sake of evaluation, a is set equal to 0.5 nm). In more narrow channels ($w < 25$ nm), an increase of E_1 in response to a decrease in w is appreciably slower than the $1/w^2$ behaviour that wide channels obey.

A qualitatively different behaviour is predicted for the dependence of the excited bound-state energy on channel width. $E_2(N)$ is a non-monotonic function. Its minimum lies at $N = 6$ (in table 1, it corresponds to the maximum of $|\Delta E_2|E_{1th}/(2|L|)$) and reaches the maximum value E_{2th} in more narrow ($N = 3$) and in infinitely wide channels. Deviations from the $1/w^2$ law are appreciable when $w \sim 50$ nm and less. The continuous model does not describe all these peculiarities of the width dependence of E_2 in ultra-narrow channels.

Just as for the ground-state energy, the characteristics of the single-mode electron transport in crossed wires are insensitive to the wire width down to $w \sim 25$ nm if the wave vector scales as k_{th}. But a further decrease of the width leads to noticeable transformations in the k_1-dependences of the scattering probabilities, which tend to be closer to the case of the crossed chains: the minimum of $R(k_1)$ and the maximum of $T(k_1)$ and $S(k_1)$ are shifting to the left, to the point $k_1 = k_{th}$. A general property of a crossed N-chain wire system is that the forward transmission is essentially improved

by enlarging the chain number from $N = 1$ to $N = 5$; if $N > 9$, the transmission becomes nearly constant.

In conclusion, we note that the approach developed here can easily be adapted to relevant 2D structures such as T-stub configurations, constrictions, double and multiple right-angle bends and similar systems. We believe that this allows a more comprehensive analysis of these systems, which are of current interest for nanoelectronics and molecular electronics.

Acknowledgments

Two of us (LM and AO) are delighted to express their gratitude to Professor V I Sugakov and his co-workers for valuable discussions of the problem.

Appendix. Scattering-amplitude equations for the continuous model of the crossed-wires system

The scattering-type solution of the Schrödinger equation (2) with the Hamiltonian $H = -\hbar^2/(2m^*)\Delta$ inside the outline in figure 1, and with an infinite potential outside this outline, has the form

$$\psi_{\mathrm{l}} = \sqrt{\frac{2}{w}}\left(\exp(ik_{j_0}x)\sin(\chi_{j_0}y) + \sum_{j=1}^{\infty} r_{k_j}\exp(-ik_j x)\sin(\chi_j y)\right)$$

$$\psi_{\mathrm{r}} = \sqrt{\frac{2}{w}}\sum_{j=1}^{\infty} t^{\mathrm{r}}_{k_j}\exp(ik_j(x-w))\sin(\chi_j y)$$

$$\psi_{\mathrm{up}} = \sqrt{\frac{2}{w}}\sum_{j=1}^{\infty} t^{\mathrm{up}}_{k_j}\exp(-ik_j y)\sin(\chi_j x)$$

$$\psi_{\mathrm{d}} = \sqrt{\frac{2}{w}}\sum_{j=1}^{\infty} t^{\mathrm{d}}_{k_j}\exp(ik_j(y-w))\sin(\chi_j x)$$

$$\psi_{\mathrm{in}} = \sqrt{\frac{2}{w}}\sum_{j=1}^{\infty}(\sin(\chi_j x)[A_{k_j}\exp(ik_j y) + B_{k_j}\exp(-ik_j y)] + \sin(\chi_j y)[C_{k_j}\exp(ik_j x) + D_{k_j}\exp(-ik_j x)]) \tag{A1}$$

where the coordinate axes x ($\rightarrow$) and y ($\downarrow$) originate from the left-hand upper corner of the intersection region, $\chi_j = \pi j/w$ and $k_{j_0}^2 + \chi_{j_0}^2 = k_j^2 + \chi_j^2$. The expansion coefficients in equation (A1) can be found by matching the wave functions $\psi_{\gamma=\mathrm{l,r,up,d}}$ and ψ_{in} and their derivatives at the boundaries of the region of intersection with all the other regions.

The condition of continuity of the wave function at the boundaries gives

$$A_{k_j} + B_{k_j} = t^{\mathrm{up}}_{k_j} \qquad C_{k_j} + D_{k_j} = \delta_{j,j_0} + r_{k_j}$$

$$\mathrm{i}(A_{k_j} - B_{k_j}) = \frac{1}{\sin(k_j w)}(t^{\mathrm{d}}_{k_j} - t^{\mathrm{up}}_{k_j}\cos(k_j w))$$

$$\mathrm{i}(C_{k_j} - D_{k_j}) = \frac{1}{\sin(k_j w)}[t^{\mathrm{r}}_{k_j} - (\delta_{j,j_0} + r_{k_j})\cos(k_j w)]. \tag{A2}$$

Equating derivatives of ψ_1 and ψ_{in} at $x = 0$, we obtain

$$i\sum_{j=1}^{\infty} k_j[\delta_{j,j_0} - r_{k_j} - (C_{k_j} - D_{k_j})]\sin(\chi_j y)$$
$$= \sum_{j=1}^{\infty} \chi_j[(A_{k_j} + B_{k_j})\cos(k_j y) + i(A_{k_j} - B_{k_j})\sin(k_j y)]. \tag{A3}$$

Excluding from equation (A3) the coefficients A_{k_j}, B_{k_j}, C_{k_j}, D_{k_j} and making use of the relations

$$\int_0^w \sin(\chi_j y)\sin(k_{j'} y)\,dy = (-1)^{j+1}\frac{\chi_j}{\chi_j^2 - k_{j'}^2}\sin(k_{j'} w)$$
$$\int_0^w \sin(\chi_j y)\cos(k_{j'} y)\,dy = \frac{\chi_j}{\chi_j^2 - k_{j'}^2}[1 + (-1)^{j+1}\cos(k_{j'} w)]$$

we find

$$\exp(-ik_j w)r_{k_j} = -\delta_{j,j_0}\exp(ik_j w) + t^{r}_{k_j}$$
$$+ 2\frac{\sin(k_j w)}{k_j w}\sum_{j'=1}^{\infty}\frac{\chi_j \chi_{j'}}{\chi_j^2 - k_{j'}^2}(t^{up}_{k_{j'}} + (-1)^{j+1}t^{d}_{k_{j'}}). \tag{A4}$$

After introducing dimensionless units $q_j = k_j w/\pi$ and notations

$$G^{c}_{j,j'} = \frac{2}{\pi}\frac{jj'}{j^2 - q_{j'}^2}$$

we finally rewrite equation (A4) as

$$\exp(-i\pi q_j)r_{q_j} = -\delta_{j,j_0}\exp(i\pi q_j) + t^{r}_{q_j}$$
$$+ \frac{\sin(\pi q_j)}{q_j}\sum_{j'=1}^{\infty} G^{c}_{j,j'}(t^{up}_{q_{j'}} + (-1)^{j+1}t^{d}_{q_{j'}}). \tag{A5}$$

The rest of the equations for r_{k_j} and $t^{\gamma}_{k_j}$ can be obtained in a similar way. The result is

$$\exp(-i\pi q_j)t^{r}_{q_j} = \delta_{j,j_0} + r_{q_j}$$
$$+ \frac{\sin(\pi q_j)}{q_j}\sum_{j'=1}^{\infty}(-1)^{j'+1}G^{c}_{j,j'}(t^{up}_{q_{j'}} + (-1)^{j+1}t^{d}_{q_{j'}}) \tag{A6}$$

$$\exp(-i\pi q_j)t^{up}_{q_j} = t^{d}_{q_j} + \frac{\sin(\pi q_j)}{q_j}G^{c}_{j,j_0}$$
$$+ \frac{\sin(\pi q_j)}{q_j}\sum_{j'=1}^{\infty} G^{c}_{j,j'}(r_{q_{j'}} + (-1)^{j+1}t^{r}_{q_{j'}}) \tag{A7}$$

$$\exp(-i\pi q_j)t^{d}_{q_j} = t^{up}_{q_j} + (-1)^{j_0+1}\frac{\sin(\pi q_j)}{q_j}G^{c}_{j,j_0}$$
$$+ \frac{\sin(\pi q_j)}{q_j}\sum_{j'=1}^{\infty}(-1)^{j'+1}G^{c}_{j,j'}(r_{q_{j'}} + (-1)^{j+1}t^{r}_{q_{j'}}). \tag{A8}$$

Equations (A5)–(A8) are exactly the same as equations (15)–(19) in the continuum limit.

References

[1] Schult R L, Ravenhall D G and Wyld H W 1989 *Phys. Rev.* B **39** 5476
[2] Sols F, Macucci M, Ravaioli U and Hess K 1989 *J. Appl. Phys.* **66** 3892
[3] Kirzcenow G 1989 *Phys. Rev.* B **39** 10452
[4] Lent S 1990 *Appl. Phys. Lett.* **57** 1678
[5] Weisshaar A, Lary J, Goodnick S M and Tripathi 1989 *Appl. Phys. Lett.* **55** 2114
[6] Berggren K-F and Ji Zhen-li 1990 *Superlatt. Microstruct.* **8** 59
Berggren K-F and Ji Zhen-li 1991 *Phys. Rev.* B **43** 4760
[7] Wu J C, Wybourne M N, Yindeepol W, Weisshaar A and Goodnick S M 1991 *Appl. Phys. Lett.* **59** 102
[8] Lifshitz I M 1947 *Zh. Eksp. Teor. Fiz.* **17** 1017, 1076
[9] Landau L D and Lifshitz E M 1963 *Quantum Mechanics* (Moscow: GIFML)